Middle Paleozoic ridge subduction in Central Beishan of southern Altaids: Evidence from geochemical, Sr-Nd and zircon U-Pb-Hf-O isotopic data of Gongpoquan volcanic rocks

Rongguo Zheng*[1, 2], Jinyi Li [1], Wenjiao Xiao [2,3,4,5]

[1] Institute of Geology, Chinese Academy of Geological Sciences, Beijing 100037, China

[2] Xinjiang Research Center for Mineral Resources, Xinjiang Institute of Ecology and Geography, Chinese Academy of Sciences, Urumqi 830011, China

[3] State Key Laboratory of Lithospheric Evolution, Institute of Geology and Geophysics, Chinese Academy of Sciences, Beijing 100029, China

[4] College of Earth and Planetary Sciences, University of Chinese Academy of Sciences, Beijing 100049, China

[5] CAS Center for Excellence in Tibetan Plateau Earth Sciences, Chinese Academy of Sciences, Beijing 100101, China

*Corresponding author

Email: rgzheng@163.com

Supplementary materials

Contents of this file

1. Supplementary Text

Text S1 Analytical methods of geochemical and geochronological data for Gongpoquan volcanic rocks.

Text S2 Detailed description of zircon U–Pb geochronology and Hf–O isotopic compositions for Gongpoquan volcanic rocks.

Text S3 Discussion for possibilities of crustal contamination in the petrogenesis of the Gongpoquan volcanic rocks.

2. Supplementary Figure

Fig. S1 Field photos and photomicrographs of the Gongpoquan volcanic rocks in the Xiaohuangshan area. a—Gongpoquan volcanic rocks are covered by marble; b—Gongpoquan volcanic rocks inject into fractures in the marble; c, d and e—Field outcrop of Gongpoquan basalt (c and e), and andesites (d); (f—j): Photomicrographs of Gongpoquan basalts (i and h), and andesites (f, g and j), showing their porphyritic textures and mineral compositions (Cpx-clinopyroxene, Pl-plagioclase, Hbl- hornblende, Q-quartz).

Fig. S2 Representive cathodoluminescence (CL) images of zircons from Gongpoquan volcanic rocks in the Xiaohuangshan area. The circles with yellow solid lines for U–Pb analysis points and the circles with red dash lines for Hf analysis points; The yellow and red numbers represent $^{206}Pb/^{238}U$ ages and $\varepsilon_{Hf}(t)$ values, respectively.

3. Supplementary Table (Files uploaded separately)

Table S1 Zircon U–Pb analytical data of Gongpoquan volcanic rocks in the Xiaohuangshan area.

Table S2 Major and trace elements compositions of Gongpoquan volcanic rocks in the Xiaohuangshan area.

Table S3 Zircon Hf and O isotopic compositions of Gongpoquan volcanic rocks in the Xiaohuangshan area.

Table S4 Whole rock Rb-Sr and Sm-Nd isotopic compositions of Gongpoquan volcanic rocks in the Xiaohuangshan area.

Text S1 Analytical methods of geochemical and geochronological data for Gongpoquan volcanic rocks

1.1 Zircon SHRIMP U-Pb analyses

Separation of zircon crystals were accomplished by conventional heavy liquid and magnetic techniques. The individual crystals were mounted in epoxy together with the TEMORA standard zircons, and then polished to approximately half their original thickness. Zircon grains were then photographed by optical microscopy, and cathodoluminescence (CL) images were obtained using a HITACHI S-3000N SEM with accelerating voltage of 10 kV and an electron current of 100 μA. U-Pb isotopic ratios of zircon crystals were measured using the SHRIMP II in the Beijing SHRIMP Center, Institute of Geology, Chinese Academy of Geological Sciences, Beijing, China. Instrumental conditions and measurement procedures are the same as those described by Compston et al. (1992). Spots of approximately 20μm-diameter were analyzed. Data for each spot were collected in sets of five scans. The $^{206}Pb/^{238}U$ ratios of the samples were corrected using reference zircon of TEMORA ($^{206}Pb/^{238}U$ = 0.06683; 417 Ma), and U concentrations were normalized using reference zircon of M257 (U=840 ppm, Nasdalaet al., 2008). The data were corrected for common Pb on the basis of the measured ^{204}Pb. The decay constants and present-day $^{238}U/^{235}U$ value given by Steiger and Jager (1977) were used. Data processing and assessment was carried out using the SQUID and ISOPLOT programs (Ludwig, 2001, 2003). Uncertainties for the isotopic ratios of individual analyses in Supplementary Table 1 and on the concordia diagrams are given at 1σ, whereas uncertainties for weighted mean ages in the text are quoted at the 95% confidence level.

1.2 Zircon LA-ICP MS U-Pb analyses

Zircon U–Pb isotopic analysis was carried out at Key laboratory of Mineral Resources Evaluation in Northeast Asia, Ministry of Land and Resources of China. The instrument couples a quadrupole ICP-MS (Agilient 7900) and 193-nm ArF Excimer laser (COMPexPro 102, Coherent, DE) with the automatic positioning system. For the present work, laser spot size was set to 32 μm for most analyses, laser energy density at 10 J/cm^2 and repetition rate at 8 Hz. The procedure of laser sampling is 30s blank, 30 seconds sampling ablation, and 2min- sample-chamber flushing after the ablation. The ablated material is carried into the ICP-MS by the high-purity Helium gas stream with flow of 1.15 L/min. The whole laser path was flushed with Ar (600m L/min) in order to increase energy stability. The counting time is 20ms for ^{204}Pb 、^{206}Pb、^{207}Pb and ^{208}Pb, 15ms for ^{232}Th、^{238}U，20ms for ^{49}Ti, and 6 ms for other elements. Calibrations for the trace element concentrations (such as U and Th) of zircon analyses were carried out using NIST 610 glass as an external standard and Si as internal standard. U/Pb ages were corrected using zircon 91500 (Wiedenbeck et al., 1995) as external standard. Zircon standard GJ-1 (603 Ma) is also used as a secondary standard to supervise the deviation of age measurement/calculation (Sláma, et al., 2008). Isotopic ratios and element concentrations of zircons were calculated using Glitter. Concordia ages and diagrams were obtained using Isoplot/Ex (3.0) (Ludwig, 2003). The common lead was corrected using LA-ICP-MS Common Lead Correction (ver. 3.15), followed the method of Andersen T., (2002). The analytical data are presented on U-Pb Concordia diagrams with 2σ errors. The mean ages are weighted means at 95% confidence levels (Ludwig, 2003).

1.3. Zircon Hf isotopic analyses

Zircon Lu-Hf isotope analyses were performed using a Thermo Finnigan Neptune MC-ICP-MS system coupled to a New Wave UP193 nm laser ablation system at the Laboratory of Isotope Geology, Tianjin Institute of Geology and Mineral Resources, Tianjin, China. Instrumental conditions and data acquisition follow those described by Geng et al. (2017). In situ zircon Hf isotopic analyses were conducted on the same spots or on the same zircon zones for the U-Pb dating. According to zircon size, ablation diameter was 50 μm or 35μm, and a laser repetition rate of 11 Hz at 100 mJ was used for ablating zircons. Heliumwas used as the carrier gas for the ablated aerosol. A common international accepted zircon standard sample GJ-1 and 91500 were used as a reference material in the experiment. Related conditions for the instruments operation and a detailed analysis procedure can be found in ref. Geng et al (2017). The $\varepsilon_{Hf}(t)$ value was calculated by assuming chondritic values of $^{176}Lu/^{177}Hf = 0.282772$ and $^{176}Hf/^{177}Hf = 0.0332$ (Blichert−Toft and Albarède, 1997). The single-stage model age (T_{DM1}) is calculated relative to the depleted mantle with a present-day $^{176}Hf/^{177}Hf = 0.28325$ and $^{176}Lu/^{177}Hf = 0.0384$ (Griffin et al., 2000). The two-stage continental crust model ages ($T_{DM\,C}$) are also calculated by plotting the initial $^{176}Hf/^{177}Hf$ of zircons back to the depleted mantle evolutionary curve using the value of $^{176}Lu/^{177}Hf$ (0.015) for the average continental crust (Griffin et al., 2000).

1.4. Whole-rock geochemical analyses

These samples were crushed after removal of weathered surfaces. The small rock chips were then pulverized into powders using an agate mortar to a grain size of ＜200 mesh. Whole-rock geochemical analyses were performed at the National Research Center of Geoanalysis, Chinese Academy of Geological Sciences, Beijing. Major elements were analyzed by X-ray fluorescence spectrometry. Ferrous iron was determined by the wet chemical titration method. Trace elements (including REE) were determined by inductively coupled plasma-mass spectrometry (ICP-MS) following the techniques of Qi and Gregoire (2000). The analytical uncertainties for major elements were generally within 1–5%. In-run analytical precision for most trace elements was better than 5%.

1.5. Whole-rock Sr-Nd isotope analyses

Whole-rock Sr and Nd isotopic ratios were measured by MC–ICP MS at the Beijing Createch Testing Technology Co., Ltd. Sample preparation and chemical separation are the same as reported by Li et al. (2012). Exponential equations were used for mass fractionation corrections for Sr and Nd isotopic ratios were based on $^{86}Sr/^{88}Sr$ = 8.375209 and $^{146}Nd/^{144}Nd$ = 0.7219, respectively. The BNVO-2 and BCR-2 standards measured during the analytical course gave $^{143}Nd/^{144}Nd$ of 0.512940 ± 6 (2σ) and 0.512626 ± 14 (2σ) values, and ave $^{187}Sr/^{86}Sr$ of 0.703499 ± 6 (2σ) and 0.705027 ± 7 (2σ) values, respectively. $^{87}Rb/^{86}Sr$ and $^{147}Sm/^{144}Nd$ ratios are calculated using the Rb, Sr, Sm and Nd abundances measured by ICP-MS. The measured and age-corrected $^{87}Sr/^{86}Sr$ and $\varepsilon_{Nd}(t)$ are listed in Table 4.

1.6. Zircon O isotopic analyses

Oxygen isotope analyses were performed on the SHRIMP II MC of the Beijing SHRIMP

Center following methods similar to those described by Ickert et al. (2008) and Wan et al. (2013). The mounts were polished lightly to remove the oxygen implanted during the U–Pb dating and re-plated with gold prior to O isotope analyses. A Cs+ beam was focused to a diameter of ~20 lm on the sample surface, with a primary intensity of ~5 nA. Positive secondary ions were accelerated by 10 kV with a normal-incidence electron gun for charge compensation. ^{16}O and ^{18}O isotopes were measured in multi-collector mode by dual Faraday cups. The data are listed in Table 3. The $\delta^{18}O$ values are referenced to the Vienna standard mean ocean water (V-SMOW), and uncertainties for individual analyses are at 2r confidence level. TEMORA was analyzed for calibration of $\delta^{18}O$ values after every 2 or 3 analyses, and measured $\delta^{18}O$ values were normalized to 8.2‰ (Black et al., 2004).

References:

Andersen, T., 2002. Correction of common lead in U–Pb analyses that do not report Pb- 204. Chemical Geology 192, 59–79.

Black, L.P., Kamo, S.L., Allen, C.M., Davis, D.W., Aleinikoff, J.N., Valley, J.W., Mundil, R., Campbell, I.H., Korsch, R.J., Williams, I.S., Foudoulis, C., 2004. Improved Pb-206/U-258 microprobe geochronology by the monitoring of a trace-element-related matrix effect; SHRIMP, ID-TIMS, ELA-ICP-MS and oxygen isotope documentation for a series of zircon standards. Chemical Geology 205 (1–2), 115–140.

Blichert-Toft, J., Albarède, F., 1997. The Lu-Hf geochemistry of the chondrites and the evolution of the mantle-crust system. Earth Planet. Sci. Lett. 148 (1–2), 243–258.

Geng, J.Z., Qiu, K.F., Gou, Z.Y., Yu, C.H., 2017. Tectonic regime switchover of Triassic Western Qinling Orogen:Constraints from LA-ICP-MS zircon U–Pb geochronology and Lu–Hfisotope of Dangchuan intrusive complex in Gansu, China. Chemie Erde – Geochemistry, http://dx.doi.org/10.1016/j.chemer.2017.05.001.

Griffin, W.L., Pearson, N.J., Belousova, E., Jackson, S.E., Van Achterbergh, E., O'reilly, S.Y., Shee, S.R., 2000. The Hf isotope composition of cratonic mantle: LAM–MC-ICPMS analysis of zircon megacrysts in kimberlites. Geochimica et Cosmochimica Acta 64, 133–147.

Hou, K.J., Li, Y.H., Zou, T.R., Qu, X.M., Shi, Y.R., Xie, G.Q., 2007. Laser ablation-MC-ICP-MS technique for Hf isotope microanalysis of zircon and its geological applications. Acta Petrologica Sinica 23, 2595–2604 (in Chinese with English abstract).

Ickert, R.B., Hiess, J., Williams, I.S., Holden, P., Ireland, T.R., Lanc, P., Schram, N., Foster, J.J., Clement, S.W., 2008. Determining high precision, in situ, oxygen isotope ratios with a SHRIMP II: Analyses of MPI-DING silicate-glass reference materials and zircon from contrasting granites. Chemical Geology 257, 114–128.

Li, C.F., Li, X.H., Li, Q.L., Guo, J.H., Li, X.H., Yang, Y.H., 2012. Rapid and precise determination of Sr and Nd isotopic ratios in geological samples from the same filament loading by thermal ionization mass spectrometry employing a single-step separation scheme. Analytica Chimica Acta 727, 54–60.

Ludwig, K.R., 2003. User's Manual for Isoplot 3.00. A Geochronological Toolkit for Microsoft Excel. Berkeley Geochronology Center, Berkeley, California. Special Publication No. 4a, 70.

Qi, L., Gregoire, D.C., 2000. Determination of trace elements in 26 Chinese geochemistry reference materials by inductively coupled plasma-mass spectrometry. Geostandard Newsletters 24, 51–63.

Sláma, J., Košler, J., Condon, D. J., Crowley, J.L., Gerdes, A., Hanchar, J.M., Horstwood, M.S.A, Morris,G.A., Nasdala, L., Norberg,N., Schaltegger, U., Schoene, B., Tubrettk, M.N., and Whitehouse, M.J., 2008. Plešovice zircon—A new natural reference material for U–Pb and Hf isotopic microanalysis. Chemical Geology 249, 1–35.

Steiger, R.H., Jäger E., 1977. Subcommission on geochronology: Convention on the use of decay constants in geo- and cosmochronology. Earth and Planetary Science Letters 36, 359–362.

Wan, Y.S., Zhang Y.H., Williams, I.S., Liu, D.Y., Dong, C.Y., Fan, R.L., Shi, Y.R., Ma, M.Z., 2013. Extreme zircon O isotopic compositions from 3.8 to 2.5Ga magmatic rocks from the Anshan area, North China Craton. Chemical Geology 352: 108–124.

Wiedenbeck M, Alle P, Corfu F, Griffin WL, Meier M, Oberli F, Vonquadt A, Roddick JC, Speigel W (1995) Three natural zircon standards for U–Th–Pb, Lu–Hf, trace-element and REE, analyses. Geostand. Newsl. 19: 1–23

Text 2 Zircon U–Pb geochronology and Hf–O isotopic compositions

U–Pb isotopic ratios and oxygen isotopic analyses of zircon crystals were measured by SHRIMP II at the Beijing SHRIMP Center. Zircon LA–ICP–MS U–Pb isotopic analyses were conducted at the Key laboratory of Mineral Resources Evaluation in Northeast Asia, Ministry of Land and Resources of China, Changchun, China. Zircon Lu–Hf isotopic analyses were performed at the Laboratory of Isotope Geology, Tianjin Institute of Geology and Mineral Resources, Tianjin, China.

Detailed descriptions of the methods used for zircon U–Pb geochronology and in situ zircon Hf and O isotopic analyse are presented in the Appendix. Representative Cathodoluminescence (CL) images of analyzed zircons are shown in Fig. 3. U–Pb dating results are listed in Table 1 and presented as concordia diagrams in Fig. 4. We also determined the Lu–Hf and O isotopic compositions of zircon grains that were analyzed during U–Pb dating. Analytical results are listed in Table 3, including $\varepsilon_{Hf}(t)$ values and model ages calculated using $^{206}Pb/^{238}U$ ages.

Zircons from Sample BS17–3 are subhedral and granular, and exhibit weak concentric oscillatory zoning indicating their magmatic origins (Fig.3). They exhibit relatively high Th (53.5–397 ppm) and U (51.4–373 ppm) abundances, and high Th/U ratios (0.40–1.40). There are two inherited zircon grains obtained with $^{206}Pb/^{238}U$ apparent ages of 496 Ma and 438 Ma. The other 22 analyses yield colse $^{206}Pb/^{238}U$ apparent ages of 410–417 Ma, with a weighted mean age of 411.2 ± 3.4 Ma (MSWD = 0.032, n = 22, Fig. 4), which is interpreted as the crystallization age. Fifteen zircon grains, which have been dated, are analyzed to obstain their Lu–Hf isotopic compositions. The ($^{176}Hf/^{177}Hf)_i$ ratios vary from 0.282674 to 0.282866. The zircon grains exhibit high positive $\varepsilon_{Hf}(t)$ values, varying from 5.62 to 12.37 (Fig.5). All the zircon grains have relatively young Hf model ages (T_{DM1}=538–807 Ma and T_{DM2}=611–1043 Ma).

Zircons from the Sample BS20–4 display euhedral-subhedral and short prismatic with length/width ratios ranging from 2:1 to 3:1. They exhibit weak concentric oscillatory zoning of magmatic origins (Figs. 4 c and d). They exhibit relatively low Th (18—90 ppm) and U (45—331 ppm) abundances, and high Th/U ratios (0.19–0.72). All the analyzed zircon grains exhibit concordant age, and eight zircon grains have older $^{206}Pb/^{238}U$ ages, and seven form a cluster with a weighted mean age of 504 ± 10 Ma (MSWD = 0.113, n = 7, Fig. 5b). 19 analyses yield close apparent $^{206}Pb/^{238}U$ ages of 430—436 Ma, with a weighted mean age of 434.3 ± 5.2 Ma (MSWD = 0.016, n = 19, Fig. 5b), which is interpreted as the crystallization age. 16 zircon grains were analyzed for Lu–Hf isotopic compositions. The ($^{176}Hf/^{177}Hf)_i$ ratios vary from 0.282259 to 0.282511. Most of zircon grains exhibit negative $\varepsilon_{Hf}(t)$ values, ranging from -8.66 to -1.48, except one zircon grain ($\varepsilon_{Hf}(t)$ = 0.36). All the zircon grains have relatively old two-stage Hf model ages (T_{DM2}), ranging from 1394 to 1958 Ma. Fifteen zircon grains were analyzed to obstain their oxygen isotopic compositions, and their measured zircon $\delta^{18}O$ values are between 8.94 ‰ and 12.18 ‰ with a weighted mean value of 10.01 ± 0.59 ‰ (n = 15).

Zircons from Sample BA11–62 are subhedral-allotriomorphic granular, with weak concentric oscillatory zoning of magmatic origin (Fig. 3). They exhibit relatively high Th (77–

217ppm) and U (79–255ppm) abundances, and high Th/U ratios (0.59–1.00). All 14 analyses yield close $^{206}Pb/^{238}U$ apparent ages of 408—426 Ma, with a weighted mean age of 415.3 ±2.7 Ma (MSWD = 1.2, n = 14, Fig. 4), which is interpreted as the crystallization age. Fourteen zircon grains from the Sample BA11–62 were analyzed to obstain their Lu–Hf isotopic compositions. The $(^{176}Hf/^{177}Hf)_i$ ratios vary from 0.282764 to 0.282919. The zircon grains exhibit high positive $\varepsilon_{Hf}(t)$ values, varying from 9.02 to 14.17 (Fig.5). All the zircon grains have relatively young one-stage Hf model ages (T_{DM1} = 471–685 Ma), and two-stage Hf model ages (T_{DM2} = 498–834 Ma). Fourteen zircon grains were analyzed to obstain their oxygen isotopic compositions, and their measured zircon $\delta^{18}O$ values are between 5.77 ‰ and 6.75 ‰ with a weighted mean value of 6.17 ±0.16 ‰ (n = 14).

Zircons from Sample BS19–1 are subhedral and granular, and exhibit weak concentric oscillatory zoning indicating their magmatic origins (Fig.3). They exhibit relatively high Th (71.5–593 ppm) and U (87.5–1074 ppm) abundances, and high Th/U ratios (0.32–1.68). All 20 analyses yield colse $^{206}Pb/^{238}U$ apparent ages of 419–441 Ma, with a weighted mean age of 427.6 ±3.6 Ma (MSWD = 0.55, n = 20, Fig. 4), which is interpreted as the crystallization age. We analyzed fourteen dated zircon grains from the Sample BS19–1 to obstain their Lu–Hf isotopic compositions. The $(^{176}Hf/^{177}Hf)_i$ ratios vary from 0.282670 to 0.282800. The zircon grains exhibit high positive $\varepsilon_{Hf}(t)$ values, varying from 5.68 to 10.42 (Fig. 5). All the analyzed zircon grains have relatively young one-stage Hf model ages (T_{DM1}=658–825 Ma), and two-stage Hf model ages (T_{DM2}= 749–1046 Ma).

Zircons from Sample BS44–1 are subhedral-allotriomorphic granular, and exhibit fan-shaped interior structure (Fig.3). They exhibit relatively high Th (36–424 ppm) and U (66–316 ppm) abundances, and high Th/U ratios (0.43–1.46), implying their magmatic origins. All the 26 analyses yield colse $^{206}Pb/^{238}U$ apparent ages of 425–433Ma, with a weighted mean age of 431.2 ± 4.4 Ma (MSWD = 0.020, n = 26, Fig. 4), which is interpreted as the crystallization age. Fifteen dated zircon grains are analyzed to obstain their Lu–Hf isotopic compositions. The $(^{176}Hf/^{177}Hf)_i$ ratios vary from 0.282624 to 0.282935. The zircon grains exhibit high positive $\varepsilon_{Hf}(t)$ values, varying from 4.26 to 15.27 (Fig.5). All the analyzed zircon grains have relatively young one-stage Hf model ages (T_{DM1}=439–877 Ma), and two-stage Hf model ages (T_{DM2}= 442–1142 Ma). Twelve zircon grains were analyzed to obstain their oxygen isotopic compositions, and their measured zircon $\delta^{18}O$ values are between 5.58 ‰ and 6.66 ‰ with a weighted mean value of 6.17 ± 0.28 ‰ (n = 12).

Zircons from Sample BA11-60 display subhedral and short-long columnar with length/width ratios ranging from 2:1 to 4:1. They exhibit no obvious concentric oscillatory zoning (Fig. 3). They exhibit relatively low Th (100–551 ppm) and U (121–455 ppm) abundances, and high Th/U ratios (0.30–1.46). All the analyzed zircon grains exhibit concordant age, and three zircon grains have older $^{206}Pb/^{238}U$ ages (576 Ma, 463 Ma and 443 Ma). Twenty-seven analyses yield close apparent $^{206}Pb/^{238}U$ ages of 417–421 Ma, with a weighted mean age of 420.5 ± 4.2 Ma (MSWD = 0.0113, n = 27, Fig. 4), which is interpreted as the crystallization age. Fourteen zircon grains were analyzed for Lu–Hf isotopic compositions. Their $(^{176}Hf/^{177}Hf)_i$ ratios vary from 0.282735 to 0.282894, and the $\varepsilon_{Hf}(t)$ values are all positive, varying from 7.98 to 13.70 (Fig. 5). All the analyzed zircon grains have relatively young one-stage Hf model ages (T_{DM1}=495–727 Ma), and two-stage Hf model ages (T_{DM2}= 534–899 Ma). Nine zircon grains were analyzed to obstain their oxygen isotopic compositions, and their measured zircon $\delta^{18}O$ values are between 5.67 ‰ and 6.71 ‰ with a weighted mean value of 6.04 ± 0.23 ‰ (n = 14).

Text S3 Possibilities of crustal contamination in the petrogenesis of the GPQ volcanic rocks.

Several inherited zircons are observed in the analyzed samples, suggesting some degree of crustal contamination. Based on CL images and ages of those inherited zircons, GPQ volcanic rocks may be contaminated by early Paleozoic rocks slightly. However, we suggest that such contamination did not play a significant role in the petrogenesis of the GPQ volcanics. Crustal contamination would cause a strong increase in LILE/HFSE ratios and $(^{87}Sr/^{86}Sr)_i$ ratios, but a decrease in $\varepsilon_{Nd}(t)$ values; however, except the BS20 series, all the other GPQ volcanic rocks exhibit high $\varepsilon_{Nd}(t)$ values (4.51–5.92) and low initial $^{87}Sr/^{86}Sr$ isotopic ratios (0.704217–0.705196). In addition, they also have depleted zircon Hf isotopic compositions with high zircon $\varepsilon_{Hf}(t)$ values. There are no obvious decrease trends in the SiO_2–$\varepsilon_{Nd}(t)$ diagrams, and no obvious correlations in some variation diagrams, such as SiO_2–Nb/La, which also rule out the possibility of significant crustal contamination. Though the BS20 series samples exhibit high $^{87}Sr/^{86}Sr$ and low $^{143}Nd/^{144}Nd$ ratios with negative $\varepsilon_{Nd}(t)$ values, there are also no obvious decrease trends in the SiO_2–$\varepsilon_{Nd}(t)$ diagrams. Moreover, La/Sm ratios are consistent with increasing Th/Nb ratios, which is different from crustal contamination trends. Therefore, significant crustal contamination could also be ruled out.

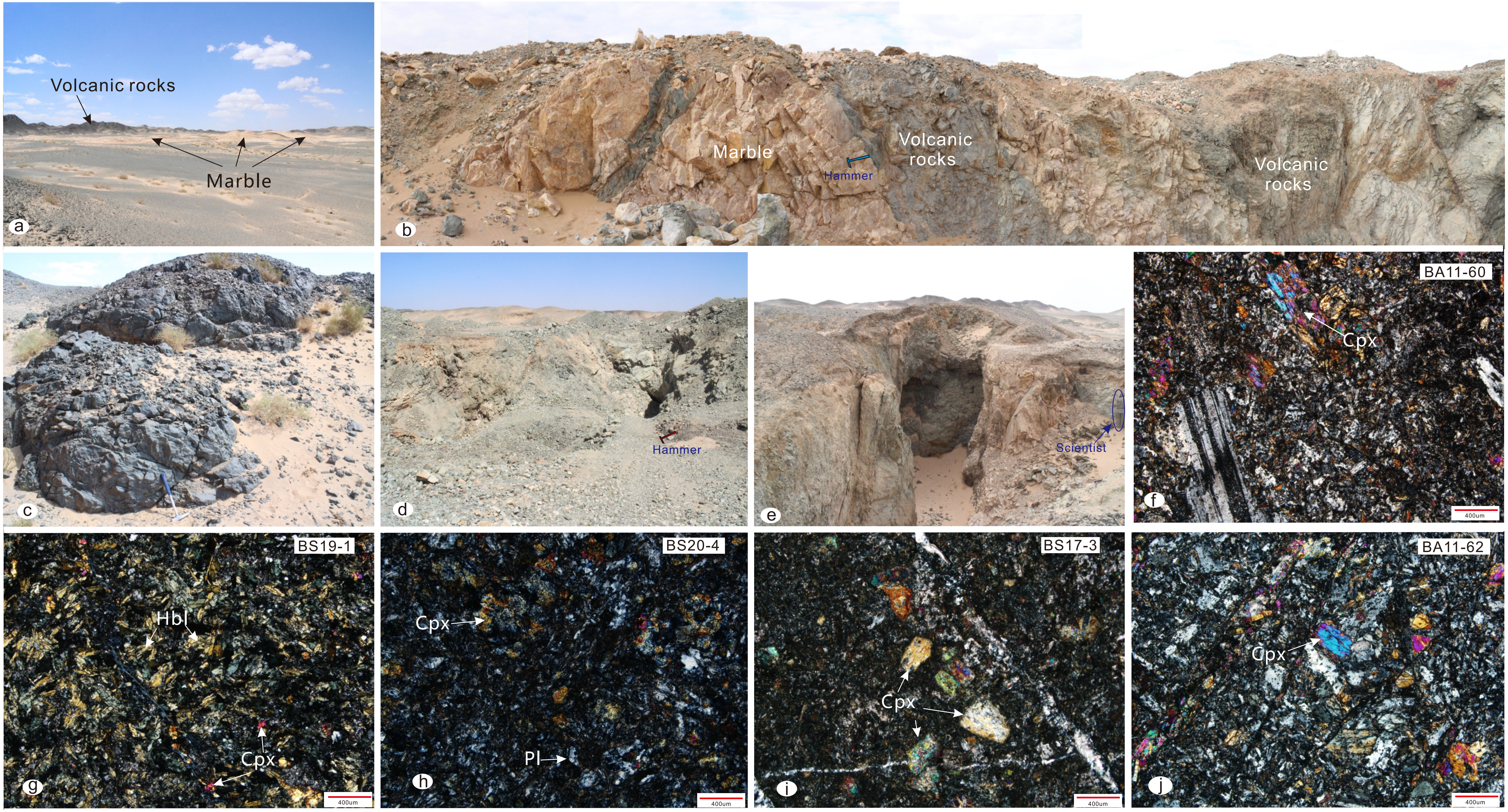

Fig. S1 Field photos and photomicrographs of the Gongpoquan volcanic rocks in the Xiaohuangshan area. a—Gongpoquan volcanic rocks are covered by marble;

b—Gongpoquan volcanic rocks inject into fractures in the marble;

c, d and e—Field outcrop of Gongpoquan basalt (c and e), and andesites (d);

(f—j): Photomicrographs of Gongpoquan basalts (i and h), and andesites (f, g and j),

showing their porphyritic textures and mineral compositions (Cpx-clinopyroxene, Pl-plagioclase, Hbl- hornblende, Q-quartz).

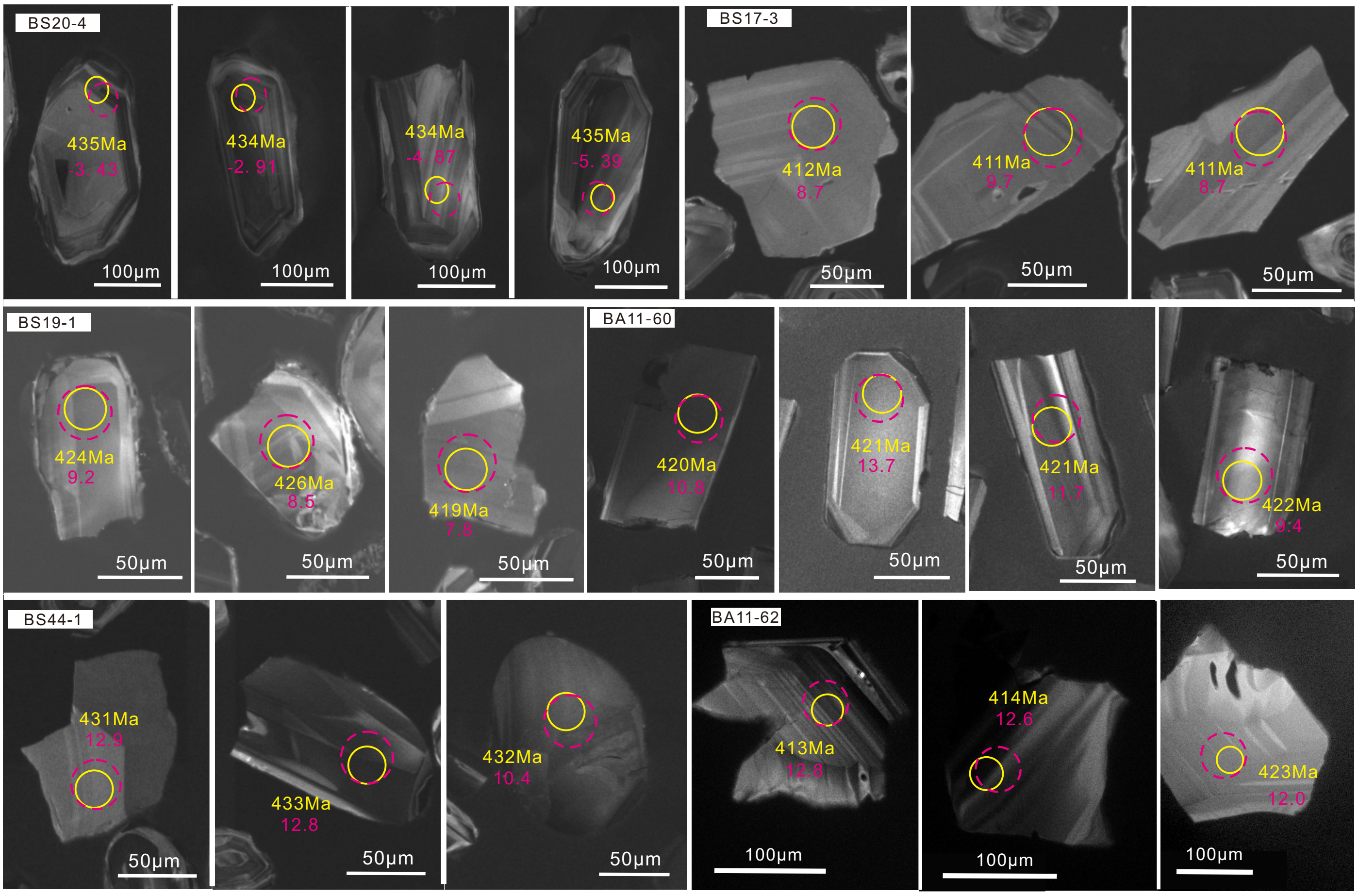

Fig.S2 Representive cathodoluminescence (CL) images of zircons from Gongpoquan volcanic rocks in the Xiaohuangshan area.

The circles with yellow solid lines for U–Pb analysis points and the circles with red dash lines for Hf analysis points; The yellow and red numbers represent $^{206}Pb/^{238}U$ ages and $\varepsilon_{Hf}(t)$ values, respectively.